ORIGINAL ARTICLE

immunology

Mast cells impair melanoma cell homing and metastasis by inhibiting HMGA1 secretion

Alberto Benito-Martin[1,2] | **Laura Nogués**[1,3] | **Marta Hergueta-Redondo**[3] | **Elena Castellano-Sanz**[3] | **Eduardo Garvin**[3] | **Michele Cioffi**[1] | **Paloma Sola-Castrillo**[1] | **Weston Buehring**[1] | **Pilar Ximénez-Embún**[4] | **Javier Muñoz**[4] | **Irina Matei**[1] | **Josep Villanueva**[5] | **Héctor Peinado**[3]

[1]Children's Cancer and Blood Foundation Laboratories, Departments of Pediatrics, and Cell and Developmental Biology, Drukier Institute for Children's Health and the Meyer Cancer Center, Weill Cornell Medical College, New York, New York, USA

[2]Universidad Alfonso X El Sabio, Facultad de Medicina, Unidad de Investigación Biomédica, Madrid, Spain

[3]Microenvironment and Metastasis Laboratory, Molecular Oncology Program, Spanish National Cancer Research Center (CNIO), Madrid, Spain

[4]Proteomics Unit—ProteoRed-ISCIII, Spanish National Cancer Research Centre (CNIO), Madrid, Spain

[5]Vall d'Hebron Institute of Oncology (VHIO), Barcelona, Spain

Correspondence
Alberto Benito-Martin, Universidad Alfonso X El Sabio, Facultad de Medicina, Unidad de Investigación Biomédica. Avenida de la Universidad 1, 28691 Villanueva de la Cañada, Madrid, Spain.
Email: albebema@uax.es

Héctor Peinado, Microenvironment and Metastasis Laboratory, Molecular Oncology Program. Spanish National Cancer Research Center (CNIO) 28029 Madrid, Spain.
Email: hpeinado@cnio.es

ABSTRACT

Metastatic disease is the major cause of death from cancer. From the primary tumour, cells remotely prepare the environment of the future metastatic sites by secreted factors and extracellular vesicles. During this process, known as pre-metastatic niche formation, immune cells play a crucial role. Mast cells are haematopoietic bone marrow-derived innate immune cells whose function in lung immune response to invading tumours remains to be defined. We found reduced melanoma lung metastasis in mast cell-deficient mouse models (Wsh and MCTP5-Cre-RDTR), supporting a pro-metastatic role for mast cells in vivo. However, due to evidence pointing to their antitumorigenic role, we studied the impact of mast cells in melanoma cell function in vitro. Surprisingly, in vitro co-culture of bone-marrow-derived mast cells with melanoma cells showed that they have an intrinsic anti-metastatic activity. Mass spectrometry analysis of melanoma-mast cell co-cultures secretome showed that HMGA1 secretion by melanoma cells was significantly impaired. Consistently, HMGA1 knockdown in B16-F10 cells reduced their metastatic capacity in vivo. Importantly, analysis of HMGA1 expression in human melanoma tumours showed that metastatic tumours with high HMGA1 expression are associated with reduced overall and disease-free survival. Moreover, we show that HMGA1 is reduced in the nuclei and enriched in the cytoplasm of melanoma metastatic lesions when compared to primary tumours. These data suggest that high HMGA1 expression and secretion from melanoma

---

Alberto Benito-Martin and Laura Nogués contributed equally to this work.

cells promote metastatic behaviour. Targeting HMGA1 expression intrinsically or extrinsically by mast cells actions reduce melanoma metastasis. Our results pave the way to the use of HMGA1 as anti-metastatic target in melanoma as previously suggested in other cancer types.

INTRODUCTION

Malignant melanoma (MM) is one of the most devastating cancers, and metastatic diseases responsible for 90% of cancer-related deaths [1]. Tumours induce the formation of pre-metastatic niches (PMN), specialized microenvironments in distant organs that are conducive to the survival and outgrowth of tumour cells [2]. PMN formation is the result of the systemic effect of tumour-secreted factors and extracellular vesicles (EVs) that facilitate the survival and outgrowth of tumour cells in target organs, collaborating with bone marrow-derived cells recruited to the metastatic site [3]. Mast cells (MCs) are haematopoietic bone marrow-derived immune cells [4] and their function in the host immune response to tumours remains to be defined [5]. MCs are broadly characterized by their content, rich in granules containing enzymes, cytokines and proteases like histamine or tryptase [6]. MCs are found in most tissues, flourishing in barrier tissues, such as skin, gut or lungs [7], and playing protective roles [8], although they are associated with allergy and anaphylaxis [9]. The role of MCs in cancer is controversial. Several studies have proposed that MCs contribute to melanoma metastasis [10], tumour growth and immunosuppression [11, 12], while others report MCs exerting anti-primary tumour effects in different cancer types [13, 14]. To interpret the dual role of MC in melanoma progression, we analysed MC function in two scenarios: (1) in vivo, analysing tumour growth and metastasis using MC-deficient models and (2) in vitro, exposing melanoma cells to bone marrow-derived MCs (BMDMCs) and re-injecting them in vivo to analyse homing and experimental metastasis formation. On the one hand, we found that, in tumour-bearing mice, MCs have a pro-metastatic activity as denoted by metastasis reduction in mast cell-deficient models. Interestingly, on the other hand, BMDMCs from wild-type (*wt*) mice have an intrinsic anti-metastatic effect when co-cultured with melanoma cells. These data support a dual role for MCs during tumour progression: an innate anti-tumoural role reducing metastatic behaviour, but once tumour progresses mast cells support metastatic spread in melanoma models. We focused on analysing the potential MCs anti-metastatic role to develop novel therapeutic strategies.

Mechanistically, MCs co-culture with melanoma cells inhibits HMGA1 secretion. HMGA1 is a nuclear protein that binds to the minor groove of AT-rich DNA strands and controls transcriptional activity of several genes [15]. Previous reports showed that increased cytoplasm expression and secretion of HMGA1 is related to metastatic behaviour in triple-negative breast cancer [16]. Ablation of HMGA1 expression in B16F10 cells decreased melanoma lung metastasis in vivo. Analysis of HMGA1 expression in human melanoma primary tumours and metastasis showed that high levels of HMGA1 expression in metastases are associated with reduced overall and disease-free survival. Finally, HMGA1 expression analysis in a cohort of 36 tumours and 12 metastatic lesions showed that cytoplasmic staining was enriched in metastatic lesions compared to primary tumours, suggesting that increased levels and cytoplasmic localization of HMGA1 are associated to metastatic behaviour in melanoma. Overall, our data support a model where HMGA1 enhances metastatic ability along melanoma progression being mobilized from nuclei to cytoplasm and secreted in melanoma cells. MCs interaction with tumour cells or HMGA1 interference reduced metastatic spread in melanoma cells suggesting that HMGA1 targeting strategies may represent a novel mechanism to reduce metastatic behaviour in melanoma.

RESULTS

Mast cells reinforce melanoma metastasis in tumour-bearing mice

To determine the role of MCs in melanoma metastasis, we subcutaneously injected (sc.i) lung metastatic B16-F10-mCherry cells in mast cell-deficient mice (Wsh). MC-deficient mice developed bigger tumours than *wt* mice as previously reported [14] (Figure 1a). However, analysis of spontaneous metastasis showed that lung metastasis was reduced in MCs-deficient mice regardless of primary tumour growth (Figure 1b). Due to reduced cell number detection, we quantified mCherry expression by immunofluorescence (Figure 1c) and qRT-PCR, observing a significant reduction of metastatic tumour
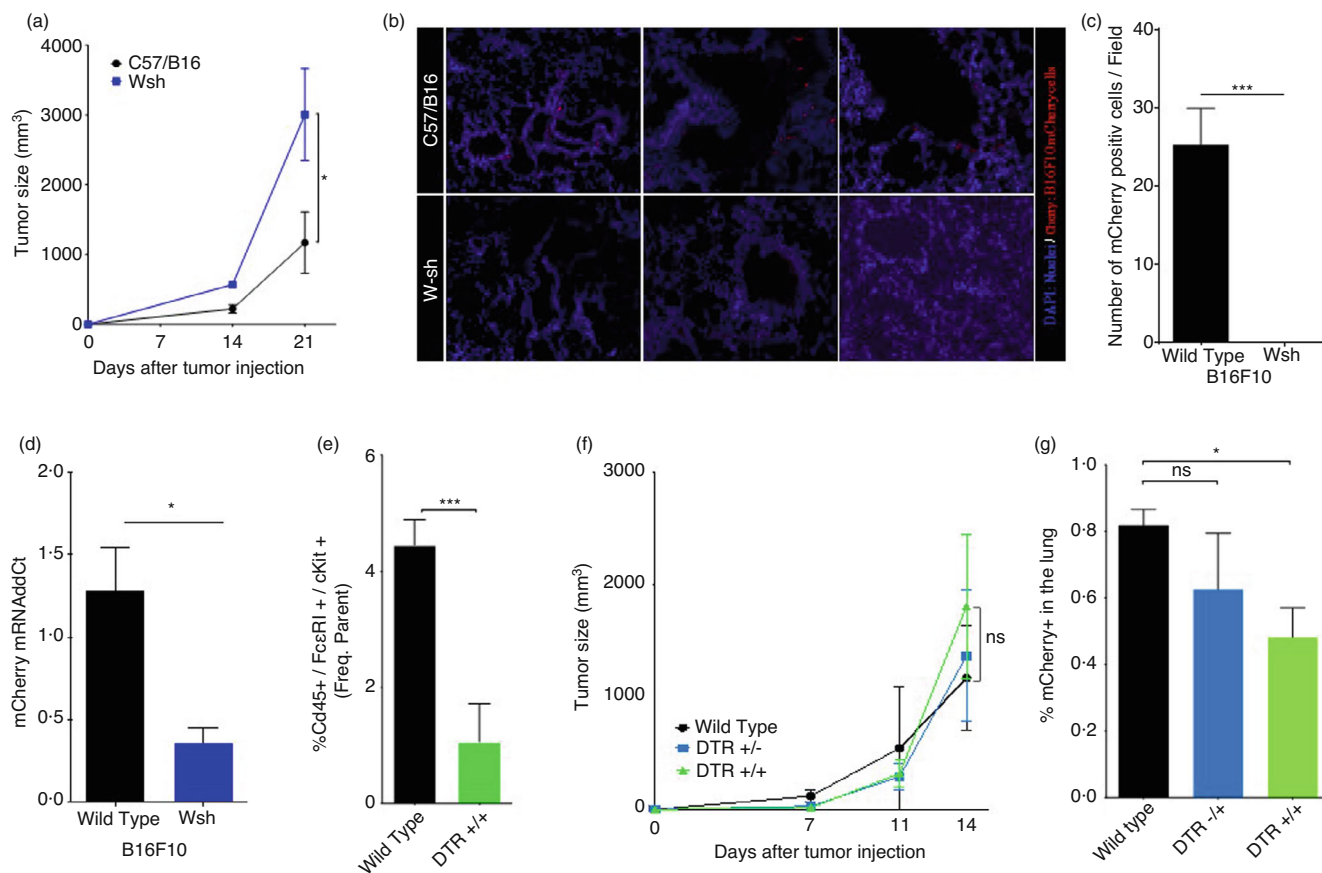
FIGURE 1 Mast cells deficiency dampens melanoma metastasis. (a) We injected B16F10-mCherry cells (1×10^6) subcutaneously in C57Bl/6 and Wsh mice and monitor tumour growth for up to 21 days. Tumour growth mean and SEM of three replicates with 3–5 mice per group and replicate. *$p < 0.05$ Parametric t-test. (b) Tumour bearing mice showed micrometastatic foci in Wsh Lungs after 21 days but not in the other groups. Three lung representative IF, showing tumour cells in red (mCherry) and nuclei in blue (DAPI) staining. First column, $10\times$. Second and third column $20\times$. All images were obtained from independent mouse samples. (c) Quantification of mCherry+ cells detected per field. $N = 6$ ***$p < 0.005$. T-test. (d) mCherry expression in mouse lungs after 21 days, detected by qPCR. *mCherry* mRNA copies in B16F10-mCherry Wsh lungs were increased when compared with C57Bl/6 mice. $N = 3$ (3–10 mice) $p < 0.05$ parametric t-test. (e) Mast cell populations in murine *wt* and MCTP5-DTR lungs detected by flow cytometry. Phenotypic characterization: Cd45+/Fcε-RI +/cKIT+.***$p < 0.005$ nonparametric t-test. (f) B16F10-mCherry cells injected (1×10^6) subcutaneously in *wt* (C57Bl/6), and MCTP5-DTR +/+ (DTR+/+) mice. MCTP5-DTR +/− (DTR+/−) mice were used as littermate controls. We monitor tumour average growth twice a week ($N = 2$, with 6–13 animals per group in total). (g) B16F10 mCherry + cells detection in *wt*, DTR +/+ and DTR+/− dissociated lungs as detected by flow cytometry. *$p < 0.05$ parametric t-test.

cells (Figure 1d). Since Wsh mice have defects in haematopoietic progenitors [17] in addition to MCs, we used an additional mouse model, the MCTP5-Cre-RDTR mouse model, deficient in connective-tissue MCs [18]. This model has been previously used to demonstrate the reduction of experimental melanoma metastasis [10], but not in spontaneous metastatic models. We first verified decreased MC numbers in lungs (Figure 1e and Figure S1B) of MCTP5-Cre-RDTR mice. We next analysed primary tumour growth and spontaneous metastasis after B16F10-mCherry sc.i. in MCTP5-Cre-RDTR (Figure 1f, g). We observed that while mice did not present primary tumour growth differences, as previously reported [10] (Figure 1f), there was a significant

reduction in spontaneous lung metastasis (Figure 1g). These data support a pro-metastatic role for MCs in tumour-bearing mice.

Bone-marrow-derived mast cells reduce melanoma cell homing and metastasis in lungs after co-incubation in vitro

Our data, together with recent reports, support MCs contribution to melanoma metastasis. During melanoma progression, MCs are influenced by tumour cells. However, there are reports showing their dual role in cancer [19] combining both pro- [20] and anti-tumour effects
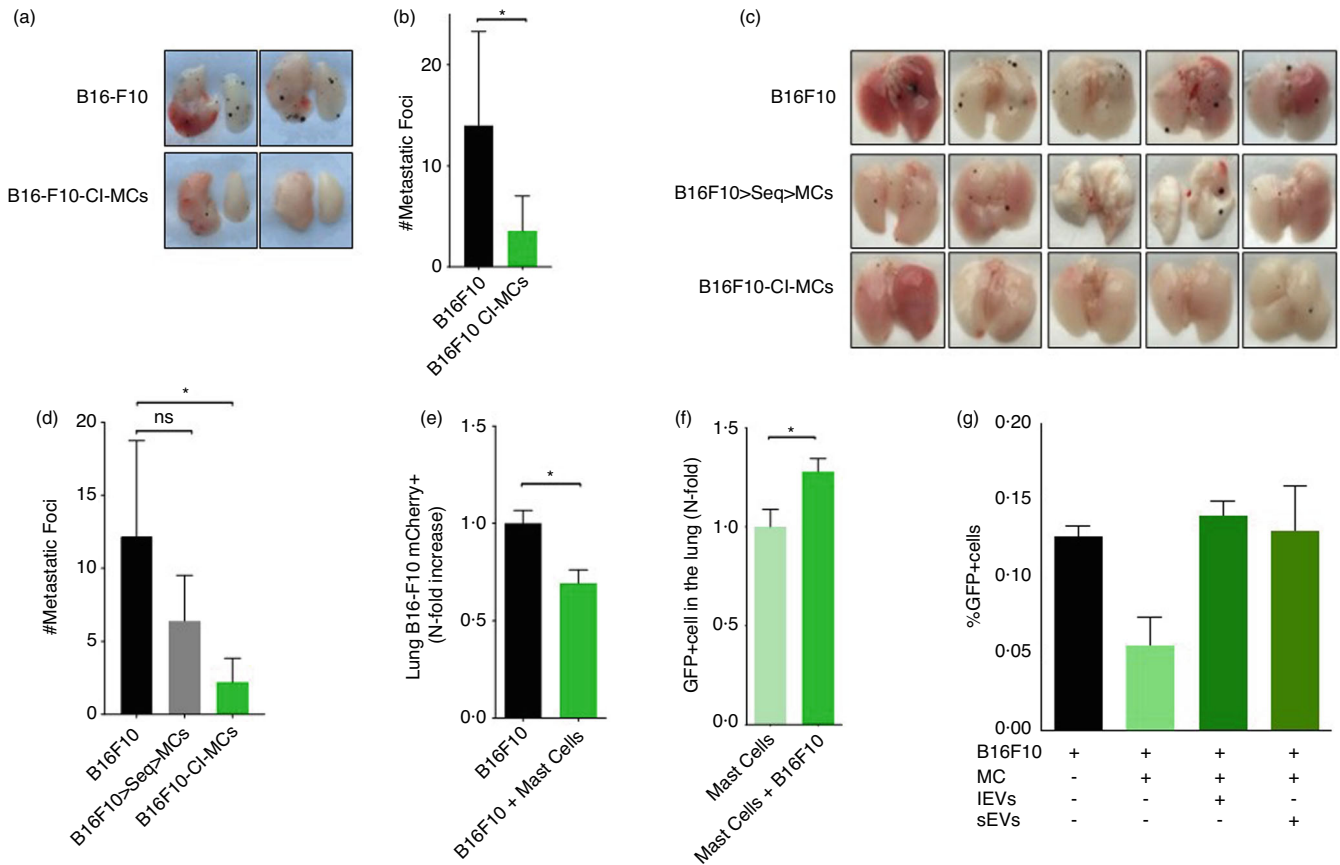
FIGURE 2 Mast cells (MCs) and melanoma coincubation reduce tumour growth and metastasis to the lung. (a) Tail vein injection of melanoma and MCs coincubation. MCs and B16F10 were coincubated (Ratio 1:1, 1×10^5: 1×10^5 cells) for 30 min and then injected in through the tail vein. Representative pictures of lungs 14 days after injection. (b) Macro-metastatic foci quantification. $N = 4$, 10–18 mice in total. *$p < 0.05$ non-parametric t-test, (c) B16F10 cells were injected in the tail vein of C57Bl/6. B16F10>Seq>MCs received two sequential injections: B16F10 and then MCs cells. The third group received an injection with the coincubation of B16F10 and MCs (Ratio 1:1, 1×10^5: 1×10^5 cells) (d) Metastatic foci quantification. $N = 5$ mice. *$p < 0.05$ nonparametric t-test. (e) Tail vein injection of melanoma and MCs coincubation after 6 h. MCs and B16F10 cells were coincubated (ratio 1:1, 1×10^6: 1×10^6 cells) for 30 min and then injected in C57Bl/6 mice. Animals were euthanized after 6 h, and lungs were processed immediately for flow cytometry analysis of mCherry detection in the lung. (f) mBMDMC-GFP Control and B16F10 cells were coincubated (ratio 1:1, 1×10^6: 1×10^6 cells) for 30 min and then injected subcutaneously in C57Bl/6 mice tail vein. Animals were euthanized after 6 h, and lungs were processed immediately for flow cytometry analysis of GFP+ cells in the lung. $N = 3$, 9 mice per group in total. *$p < 0.05$ nonparametric t-test. (g) MCs GFP+ detection in lung. B16F10 cells were coincubated with MCs (ratio 1:1, 1×10^6: 1×10^6 cells) or treated with 10 μg of large and small EVs for 30 min and then injected subcutaneously in C57Bl/6 mice tail vein. Animals were euthanized after 6 h, and lungs were processed immediately for flow cytometry analysis of mCherry detection in the lung.

[21, 22]. To understand the innate role of MCs we used bone marrow-derived cells from *wt* mice, characterized phenotypically in Figure S2A, and analysed their influence in melanoma cell behaviour. We co-incubated (CI) in vitro B16F10 melanoma cells with murine BMDMCs in a 1:1 ratio for 30 min, injecting then the mix intravenously. Surprisingly, while B16F10 control cells form macrometastasis in the lung 14 days after the injection, the CI of B16F10 with BMDMCs significantly reduced lung metastasis (Figure 2a, b). To understand if CI was necessary to reduce metastatic ability of melanoma cells, we injected the same amount of melanoma cells and BMDMCs sequentially

without previous CI (Figure 2c, d). We observed that sequential injection in vivo did not significantly reduce lung metastasis, but co-incubation did (Figure 2d). In order to analyse the mechanism involved, we evaluate cell death, but we did not detect any significant changes in apoptosis (Figure S3).

We next analysed if tumour cell homing in the lungs was affected by CI. We evaluated tumour cell presence in lungs 6 h after intravenous injection. We observed a significant reduction of tumour cell homing after CI with BMDMCs (Figure 2e, Figure S4A). We also observed an increase of GFP+ BMDMCs in the lungs in this
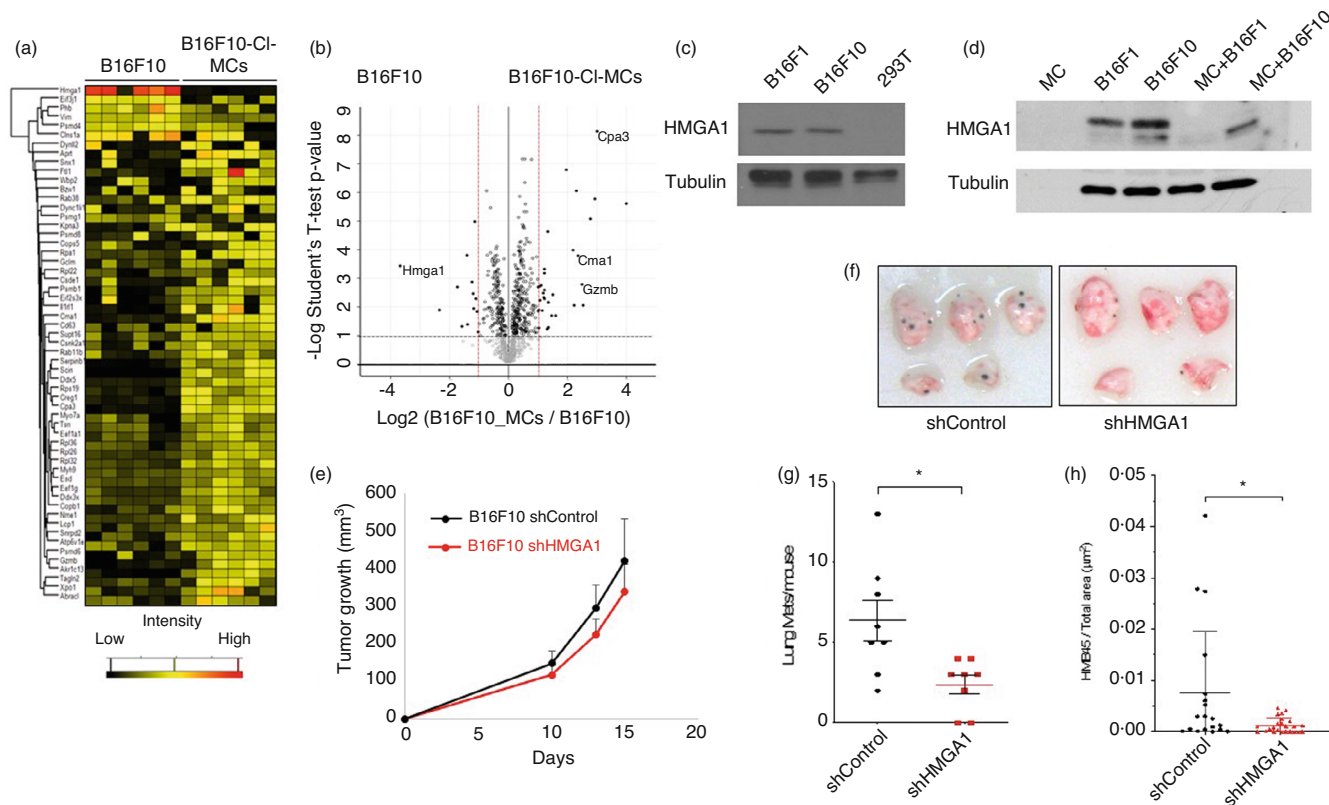
FIGURE 3 Melanoma and MC coincubation identify HMGA1 as a melanoma metastasis driver. (a) Proteomic analysis of melanoma secretome. B16F10 and B16F10-CI-MCs coincubation secretome was analysed by quantitative proteomics. We show 57 significantly regulated proteins. Among them, HMGA1 is the most abundant protein in B16F10 secretome, being almost absent in the CI secretome. (b) Volcano plot representing the 57 significantly regulated proteins comparing B16F10 and B16F10-CI-MCs secretomes. HMGA1 is highly expressed in B16F10 secretome. Typical mast cells proteins are present in the coincubation secretome, as chymase (CMA1) or mast cell Carbopeptidase (CPA3). (c). Representative Western blot for HMGA1 expression in murine melanoma cell lines. (d) Representative Western blot of the concentrated secretome of melanoma cell lines and coincubation with MCs. MCs, B16F1, B16F10 and coincubation of MCs and B16F1 or B16F10 were resuspended in PBS, and incubated for 30 min at RT. Then, supernatant was concentrated and the whole reduced volume was analysed by WB. (e) B16F10 tumour growth; 1×10^6 cells (B16F10 shControl or B16 shHMGA1) were sc injected in 8–10-week-old Bl/6 mice. Tumours were measured with a calliper three times a week. $N = 8$ mice per group. (f) B16F10 shControl and B16F10 shHMGA1 (1×10^5) cells were injected intravenously in an experimental metastasis model, observing a decrease in metastatic foci in the B16F10sh HMGA1 injected animals. Representative image of lungs is depicted ($n = 8$). (g) Lung macrometastases quantification from (f) after 14 days post injection. (h) HMB45 staining quantification of lung tissue obtained from experimental metastasis model showed in (f).

experimental setting (Figure 2f and Figures S2b, S4b), suggesting that BMDMCs colonize the lung microenvironment reducing tumour cell homing. To test if besides physical interaction during the CI, MC-secreted factors could be involved in this effect, we investigated of the capacity of MC-derived extracellular vesicles (EVs) to inhibit melanoma metastasis. Co-injection of tumour cells with MC-derived large EVs (lEVs) and MC-derived small EVs (sEVs) did not affect tumour cell homing (Figure 2g). Therefore, our data support the idea that tumour-BMDMCs co-incubation in vitro impairs tumour cell homing and metastasis through direct contact effect rather than secreted factors.

HMGA1 reduction in melanoma cells diminish metastatic behaviour

To define the mechanism involved, we analysed the secretome before and after melanoma cells- BMDMC CI. Proteomic profiling of secreted factors revealed 57 proteins significantly altered in the secretome after co-incubation of B16F10 with BMDMC (Figure 3a, b). Out of the many candidates, HMGA1 secretion was the top protein significantly downregulated after co-incubation with BMDMCs (Figure 3a, b). Since the HMG protein family is associated with cancer and tumour progression [23], we analysed the role of HMGA1 in melanoma. First,
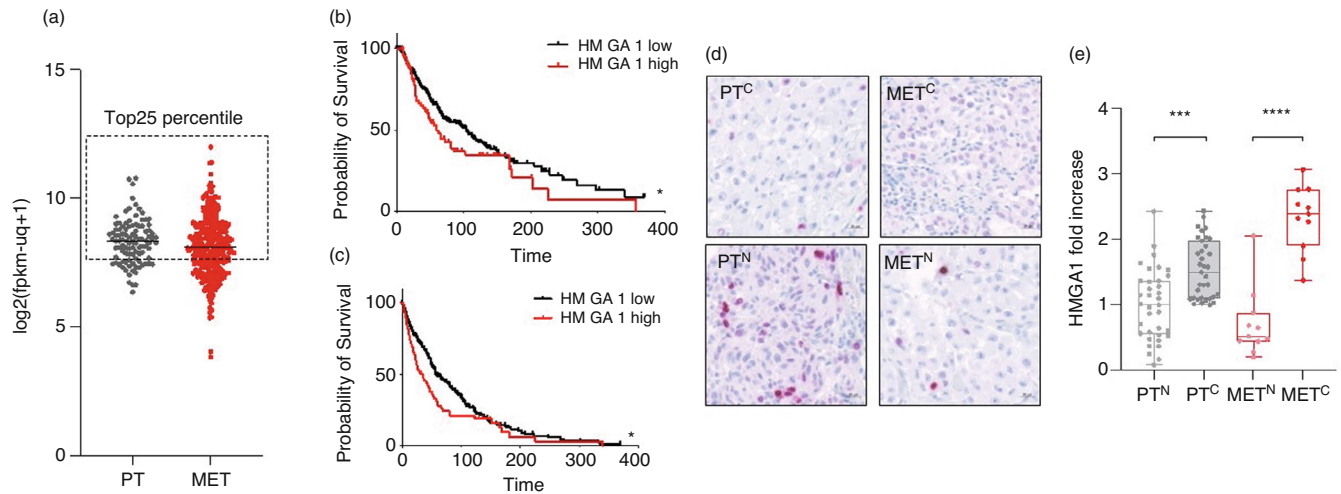
FIGURE 4 HMGA1 expression in human metastatic tissue correlated with poor prognosis. (a) Tumour and metastatic melanoma samples with the top 25% expression levels of *HMGA1* gene ('high') pointed with dashed square. Metastatic samples with the top 25% expression levels of *HMGA1* gene ('high') show significantly worse prognosis than the remaining metastatic samples ('low'). (b) Overall and (c), distant metastasis-free survival curves in melanoma metastatic samples expressing (top 25%) *HMGA1* from the TCGA dataset. Kaplan–Meier survival curves were generated and differences in OS and DFS survival were assessed by log–rank Mantel–Cox test using GraphPad PRISM 8.1.1. Analyses were performed in the TCGA datasets with all tumours (101 primary tumours and 339 metastasis). (d) Representative immunohistochemistry staining for HMGA1 in human melanoma. PTc, primary tumor citoplasmatic; PTn, primary tumor nuclear; METc, metastasis citoplasmic; METn, metastatic nuclear. (e) Tissue microarray quantification. Subcellular HMGA1 localization in 53 different primary tumors and metastatic lesions. ANOVA comparision ***$p < 0.0005$; ****$p < 0.0001$

we analysed HMGA1 expression in a panel of mouse and human melanoma cells, we found that HMGA1 was expressed in B16F1 and B16F10 mouse melanoma cells (Figure 3c) as well as in the human cells analysed (Figure S5). Next, we confirmed the reduction of HMGA1 secretion after CI with BMDMCs in B16F1 and B16F10 (Figure 3d). Due to the reduction of metastasis observed concomitantly with HMGA1 secretion by CI, we hypothesized that HMGA1 may have a pro-metastatic role in melanoma. HMGA1 has been involved in metastasis in several types of cancer [16, 24, 25], however, its role in melanoma remains undefined. To get further insights, we knocked down (KD) HMGA1 expression in B16F10 (Figure S6A), observing that HMGA1 KD does not affect B16F10 proliferation in vitro (Figure S6B) or tumour growth in a subcutaneous injection experimental model (Figure 3e). Next, we analysed the effect of HMGA1 KD in the metastatic ability by performing experimental metastasis assays after intravenous injection. We analysed metastasis macroscopically 14 days after injection and found that interference of HMGA1 in B16F10 (B16F10-shHMGA1) reduced both the number and size of lung metastases (Figure 3f, g). We also analysed metastatic dissemination in the lungs staining with HMB-45, a bona fide melanoma marker [26], and found that HMGA1 downregulation significantly reduced B16F10

cells metastatic dissemination, supporting a pro-metastatic role for HMGA1 in melanoma (Figure 3h).

HMGA1 cytoplasmic expression in metastatic lesions correlates with reduced overall survival in melanoma patients

Human HMGA1 expression promotes tumour invasion and metastasis in several cancer types [23], however, the role in melanoma is unknown. Therefore, we decided to analyse in detail the expression of HMGA1 in human melanoma. First, we analysed *HMGA1* expression in the Cancer Genome Atlas (TCGA) and we did not find significant differences in *HMGA1* expression in metastatic tissue (met) when compared with primary tissues (PT) (Figure 4a). However, we found that high *HMGA1* expression (top 25% expression) in metastatic lesions correlates with reduced overall (Figure 4b) and disease-free survival (DFS) (Figure 4c). HMGA1 has an impact on tumour metastasis in other cancer models such as breast cancer. Change from nuclear to cytoplasmic localization of HMGA1 has been used as a surrogate marker of extracellular secretion and predicts the aggressiveness of TNBC primary tumours [16]. Thus, we decided to evaluate HMGA1 subcellular localization in 51 different

primary tumours and metastatic lesions. We first confirmed that we were able to differentiate between cytoplasmic and nuclear HMGA1 localization, focusing on the cellular distribution of the signal (Figure S7) and quantified the relative abundance in these regions (Figure 4d). Analysis showed that cytoplasmic staining was increased by 4-fold in metastatic lesions compared to 1.5-fold increase shown in primary tumours (Figure 4e). These data suggest that nuclear localization of HMGA1 is reduced in metastatic lesions, concomitantly with an increase in cytoplasmic localization and potential secretion.

DISCUSSION

Melanoma metastasis is responsible for 90% of melanoma-related deaths, and new approaches are urgently needed to reduce its mortality [1]. Recently, new findings connected tumour-derived signals with PMN formation and the role of local and recruited immune cell populations in this process [2]. Mast cells, present in most barrier tissues, are innate immunity cells with a controversial role in cancer [5, 19]. Different reports have addressed the role of MCs in skin cancer, from their role in tumour growth [14] to their implication in metastasis to the lung [10]. We have observed that MC-deficient mice (Wsh) present an increase in melanoma tumour growth consistent with results reported in other skin cancer models. However, we did not observe this tumour growth increase in the MCTP5-RDTR mast cell-deficient model. This difference in tumour growth could be attributed to Wsh mice aberrant myelopoiesis due to their mutation in the *cKit* gene [12]. On the other hand, we have observed reduced metastasis in both models. Ablation of mast cells in the MCTP5-RDTR model reduced melanoma metastasis in experimental models [10], consistent with our spontaneous metastasis results in the Wsh MC-deficient mice. In a different report, mice in which with three mast cell proteases were genetically ablated showed increased lung metastasis and reduced immune recruitment to the metastatic site [27]. Therefore, it is still unclear the specific role of MCs in melanoma metastasis. Our results support a role of MCs in tumour progression, supporting the idea that MCs contribute to metastatic dissemination depending on the context. We investigated how MCs influence melanoma metastatic cell behaviour. We observed that when melanoma cells are co-incubated with MC derived from *wt* mice in experimental metastasis models, there was a reduction of lung metastasis suggesting that co-incubation somehow reduces metastatic ability. Analysis of secreted factors after co-incubation showed that secretion

of HMGA-1 by melanoma cells is reduced, suggesting a role for this factor in melanoma metastasis. HMGA1 is a chromosomal protein that binds to the minor groove of DNA and controls transcriptional activity [28]. HMGA proteins are expressed at high levels during embryogenesis, but have low or undetectable levels in most adult tissues [29]. HMGA1 overexpression has been correlated with metastasis and reduced patient survival in breast cancer [30], hepatocellular carcinoma [24] and pancreatic cancer [31]. Importantly, it was recently demonstrated that HMGA1 is secreted by invasive breast cancer cells mediating cell migration, invasion and metastasis [16]. However, the role of HMGA1 in melanoma metastasis is not defined. Our data show how co-incubation of melanoma and BMDMCs reduce melanoma metastasis and HMGA1 secretion. Reduction of HMGA1 expression in B16F10 cells reduced melanoma metastasis suggesting a role in melanoma progression. To determine the relevance in human melanoma, we analysed HMGA1 expression and subcellular localization in primary tumour and metastatic lesions, showing that high expression of HMGA1 in metastatic tissue is associated with decreased overall survival. Moreover, the analysis of the subcellular localization of HMGA1 in an additional cohort of melanoma primary tumours and metastasis showed a significant increase in cytoplasmatic HMGA1 expression. Importantly, increased cytoplasmic localization and secretion of HMGA1 have been previously associated with increased metastatic behaviour in triple negative breast cancer [16], suggesting that a similar model might happen in melanoma. Here we present the first evidence that HMGA1 plays a role in melanoma metastatic behaviour and that BMDMCs execute an anti-tumour response by inhibiting its secretion by co-incubation with tumour cells. We present evidence that reducing levels of HMGA1 in melanoma cells can indeed reduce their metastatic behaviour. Therefore, therapeutic strategies targeting HMGA1 in melanoma cells could represent novel approach to reduce melanoma metastasis.

MATERIALS AND METHODS

TCGA data analysis

To determine the clinical value of HMGA1 expression in human melanoma samples, we retrieved the gene expression data and its associated clinical information of the study from the TCGA network. GDC TCGA Melanoma (SKCM) data were extracted from cBioPortal: http://www.cbioportal.org/. The normalized expression of HMGA1 was available for 440 melanoma samples: 101 primary tumours, 339 metastases. For *HMGA1* gene,

normalized expression was categorized as 'High expression' when it was above the third quartile (top 25% expression) of all tumour and metastatic samples; otherwise, it was categorized as 'low'. Kaplan–Meier estimates of *HMGA1* expression (assessed separately for each stratum) were plotted and compared to overall survival (OS), DFS curves using log-rank and Chi-square tests.

Tumour samples

Briefly, this study was performed in two independent data samples: discovery series, which included 51 MMs, and validation series composed by 6 malignant primary tumour melanoma and their correspondent metastasis. Tissue microarrays containing 53 melanoma and metastatic samples (15 of them including non-tumoural paired tissue) and associated data used in this Project were provided by the CNIO-Biobank (B.000848) after the appropriate ethic approval. This study was approved by the local ethical committee from each institution, and a complete written informed consent was obtained from all patients.

Immunohistochemistry

HMGA1 expression and subcellular localization were analysed by immunohistochemistry (IHC) in TMAs and in PDXs, according to standard methods as previously published [18]. HMGA1 monoclonal antibody was generated as previously described [18], and HMGA1 expression was classified as positive when more than 10% of tumour cells showed positive staining. Cytoplasmic and nuclear staining of HMGA1 was quantified analysing the percentage of positive immunolabelled cells over the total cells in each tissue area Also, the overall percentage of positive cells was recorded, as well as the pathologist's semiquantitative estimate of the overall staining intensity (0–3+). The cases were also designated as 'positive' if more than 10% of the tumour cells showed expression of the antigen. All studied tumour sections also included normal tissue as an internal control. In negative controls, the primary antibodies were omitted.

Mice

C57BL/6 females (C57), C57BL/6-Tg (CAG-EGFP) 131Osb/LeySopJ (GFP mice) and B6.Cg-KitW-sh/HNihrJaeBsmJ (W-sh) of 8–12-week-old were purchased from the Jackson Laboratory. Wsh mice present embryonic deficit and eventual abolishment of mast cells soon after birth. Dr. Axel Roers kindly provided MCPT-5 Cre-R-DTA mice (MCTP5 DTR +/+) [19] which lack connective tissue mast cells. We used MCPT-5 Cre-R-DTA heterozygous (MCTP5 DTR +/−) mice as controls. For primary tumour growth and spontaneous lung metastasis experiments, we injected 1×10^6 B16F10 mCherry, B16F10shControl or B16F10shHMGA1 cells subcutaneously in the mice right flank. We monitored tumour growth at least thrice a week. Metastasis was evaluated by mCherry expression in the lung after 2 or 3 weeks. For education experiments, we injected a total of 10 µg of EVs every 72 h for 2 or 3 weeks in the eye sinus. Synthetic unilamellar 100 nm liposomes (Encapsula Nanoscience) or PBS were used as 1 controls in all studies. For lung colonization experiments, 1×10^6 B16F10–mCherry cells were injected intravenously, and C57BL/6 female mice were euthanized after 6 h. For experimental metastasis, we injected 1×10^5 B16F10–mCherry cells intravenously, and C57BL/6 female mice were euthanized after 2 weeks. Animals were sacrificed and tumour and lung samples were dissected and frozen at $-80°C$ in O.C.T. All mouse work was performed in accordance with institutional, IACUC and AAALAS guidelines. All animals were monitored for abnormal tissue growth or ill effects according to AAALAS guidelines and we euthanized animals if excessive health deterioration was observed.

Melanoma cell lines

B16F10 and B16F1 were purchased from ATCC. B16F10-mCherry cells were generated as previously described. All melanoma cells were grown in DMEM supplemented with 10% (v/v) sEV-reduced foetal bovine serum (FBS) glutamine 2 mM and antibiotics. Human melanoma cells were kindly provided by Marisol Soengas from CNIO.

Tissue processing

Specimens were fixed in 4% PFA. For immunofluorescence, 12 µm O.C.T. tissue sections of lungs were treated with PBS-0.3% triton X-100 for 15 min. Non-specific sites were blocked by incubation in PBS containing PBS 1% BSA 5% and specific Serum – 0.05% triton X-100 for 1 h at RT. We incubated primary antibody, anti-mCherry (ab167453, Abcam), overnight at 4°C. After washes with PBS, lungs were incubated 1 h with secondary antibodies from Alexa Fluor series from Molecular Probes (dilution 1:500) and washed again. Finally, samples were mounted with Prolong-DAPI (Thermo). Fluorescent images were obtained using a Nikon confocal microscope (Eclipse TE2000U) and analysed using Nikon software (EZ-C1 3.6).

Flow cytometry analysis

For lung population analysis, tissues were minced and then digested at 37°C for 20 min with an enzyme cocktail (collagenase A, dispase and DNaseI, Roche Applied Science). Single-cell suspensions were prepared by filtering through a 70-μm strainer and passing through a nylon mesh. We eliminate red blood cells with ACK lysis buffer (Gibco), and then cell suspensions were washed in Flow buffer (PBS, 5 mM EDTA and 1% BSA) and incubated with the following primary antibodies: anti-mouse CD45 (Brilliant Violet 570, 30-F11, 1:200, Biolegend), anti-mouse Fce-R1 alpha (PE-Cyanine7, MAR-1, eBioscience™ 1:400), anti-mouse cKIT (APC/Cy7,2B8, 1:200, Biolegend), anti-mouse Lineage Cocktail (1:300, Biolegend), APC anti-mouse CD63 (1:100, Biolegend), Mouse IL-3 R alpha /CD123 PerCP-conjugated Antibody (1:200, R&D systems), Mouse IL-3R beta Antibody (1:100, R6D systems), CD13 Rat anti-Mouse, Brilliant Violet 711, Clone: R3-24211 (1:200, BD Optibuild). To assess cell viability, we used LIVE/DEAD™ Fixable Violet Dead Cell Stain Kit, for fixed cells (Thermo, L34963) and Pacific Blue™ Annexin V Apoptosis Detection Kit with 7-AAD, (Biolegend, 640 926). For in vitro experiments, adherent cells were treated with cell dissociation buffer (Gibco) and single-cell suspensions were washed in Flow buffer prior to primary antibody incubation. GFP+ & mCherry+ presence in the lung were analysed using a FACSCalibur or a FACSCanto (Beckton Dickinson). FACS data was analysed with FlowJo software (TreeStar Inc.).

Quantitative PCR

We isolated RNA from frozen lungs using Qiagen RNeasy Mini Kit, to then perform reverse transcription (SuperScript™ VILO™ cDNA Synthesis Kit, Thermo) and quantitative PCR for specific gene expression using pre-designed TaqMan® assays (Thermo). *GFP* and *mCherry* expression was assessed using specific primers and SybrGreen PCR reagents (Applied Biosystems). Quantitative real-time PCR (QRT-PCR) was performed on a 7500 fast real-time PCR system (Applied Biosystems). Relative expression was calculated following delta–delta Ct calculation method and *Beta-Actin* and *18 s* were used as housekeeping genes.

Ex vivo mast cell differentiation

Bone-Marrow-derived mast cells were obtained after flushing tibia and femur from C57Bl6 (mBMDMCs) and C57BL/6-Tg (CAG-EGFP)131Osb/LeySopJ (mBMDMCs-GFP) as previously described. Briefly, bone marrow progenitors were cultured in OPTIMEM supplemented with sEV-reduced FBS and 5 ng/ml of interleukin-3 for 4 weeks. We maintained cell density at 6×10^5 cells/ml and evaluate cKIT and FcE-R1 expression weekly to validate differentiation.

Extracellular vesicle isolation

We performed small extracellular vesicle (sEV) isolation by sequential ultracentrifugation. Cells were cultured in media supplemented with 10% sEV-reduced FBS (FBS, Hyclone). FBS was reduced of bovine sEVs by ultracentrifugation at $100\,000 \times g$ for 70 min. Supernatant fractions collected from 72 to 96 h cell cultures were pelleted by centrifugation at $300 \times g$ for 5 min and $500 \times g$ for 10 min. The supernatant was centrifuged at $12\,000 \times g$ for 20 min, and the pellet collected for large EV analysis. sEVs were then harvested by centrifugation of previous step supernatant at $100\,000 \times g$ for 70 min. The sEV pellet was resuspended in 20 ml of PBS and collected by ultracentrifugation at $100\,000 \times g$ for 70 min. All spins were performed at 10°C in Beckman instruments.

Coincubation experiments and secretome analysis

The same number of mBMDMCs and B16F10 cells (1×10^6) were pelleted down and washed with PBS. After washing, cell pellets were resuspended in 500 μl of PBS and mixed for coincubation for 30 min at RT. The conditioned media were centrifuged at $300 \times g$, 5 min; $500 \times g$, 10 min and $3000 \times g$, 20 min. Conditioned media was frozen for proteomic analysis or was concentrated using a 10 000 MWCO Millipore Amicon Ultra (Millipore) to further evaluate secretome protein expression.

Western blot

Whole cell lysates and conditioned media were resolved by SDS-PAGE and Western blot analysis was performed with the following primary antibodies: rabbit anti-HMGA1 (sc-393 213, Santa Cruz Biotechnology), mouse anti-alpha-tubulin (α-tubulin [B-7]: sc-5286), β-actin (Sigma Aldrich, #A5441). Mouse m-IgGκ BP-HRP (sc-516 102, Santa Cruz Biotechnology) and Peroxidase conjugated AffinityPure donkey anti-Rabbit or anti-Mouse (1:5000, Jackson ImmunoResearch, #711-035-152 and 1:5000, #715-035-150, respectively) were used as

secondary antibodies. ECL Western Blotting Substrate (GE Healthcare) Kit was used for western blot developing. The intensities of the immunoreactive bands were quantified by densitometry using ImageJ software (NIH).

Proteomic analysis of the secretome

Samples were lysed in urea and digested with Lys-C/trypsin using the standard FASP protocol. Peptides were analysed by LC–MS/MS analysis using an LTQ Orbitrap Velos mass spectrometer (Thermo Scientific). Raw files were analysed with MaxQuant against a mouse protein database and the MaxLFQ algorithm was used for label-free protein quantification. The MS proteomic data have been deposited to the ProteomeXchange Consortium via the PRIDE partner repository with the dataset identifier PXD009505. For peer reviewing purposes, the data set can be available under the username reviewer_pxd034005@ebi.ac.uk and password: RySIl4Q1.

Lentiviral HMGA1 knock-down

To stably knockdown HMG-I/HMG-Y we used lentiviral particles (Santa Cruz Biotechnology) either containing 3 target-specific shRNA targeting mouse HMG-I/HMG-Y (sc-37116-V) or control shRNA lentiviral particles targeting a scramble sequence (sc-108080). B16F10 cells were infected overnight with lentiviral particles in the presence of polybrene (Sigma, TR-1003). Stable cell lines were obtained after 1-week selection with puromycin and HMGA1 depletion was confirmed by immunoblot. Antibodies: HMGA1 (Santa Cruz Biotechnology, sc-393 213; 1:1000) and β-ACTIN (Cell Signalling, 4967; 1:5000) overnight at 4°C. For HMGA1, m-IgGκ BP-HRP (Santa Cruz Biotechnology) was used as secondary antibody. For quantification, the ratio between the HMGA1 and β-ACTIN band intensities for each sample was measured using ImageJ software.

In vitro proliferation assay

A 1000–2000 B16F10 shControl or ShHMGA1 cells were plated on several T96 well plates by quadruplicates. The following day (Time 0) and every 24 h (times 24, 48 and 72 h), one plate was fixed for 15 min using glutaraldehyde 1% and washed with PBS twice. All plates were then stained with 100 μl/well of Crystal Violet 0.25% (in H_2O) for 1 h at room temperature. After discarding the remaining Crystal Violet, plates were washed 4–5 times with H_2O and dried over night. A 100 μl of acetic acid (15%) was

added to each well and incubated 1 h at room temperature with gently shaking. Absorbance was read at 590 nm and all measurements were referred to time 0.

Statistical analysis

Error bars in graphical data represent means ± SEM. Mouse experiments were performed at least triplicate, using at least 5 mice per treatment group, except noted. All in vitro experiments were performed at least in duplicate. Statistical significance was determined using parametric and nonparametric t-tests. p-Values of $p < 0.05$ were considered statistically significant using GraphPad Prism software.

CNIO, certified as Severo Ochoa Excellence Centre, is supported by the Spanish Government through the Instituto de Salud Carlos III (ISCIII).

CONFLICT OF INTEREST

The authors declare no conflict of interest.

DATA AVAILABILITY STATEMENT

The data that support the findings of this study are available from the corresponding author upon reasonable request.

ORCID

Alberto Benito-Martin https://orcid.org/0000-0002-0700-3891
Laura Nogués https://orcid.org/0000-0002-7592-4430
Elena Castellano-Sanz https://orcid.org/0000-0002-0851-129X
Michele Cioffi https://orcid.org/0000-0003-4180-5369
Paloma Sola-Castrillo https://orcid.org/0000-0003-1554-0344
Weston Buehring https://orcid.org/0000-0003-0946-0671

REFERENCES

1. Garbe C, Amaral T, Peris K, Hauschild A, Arenberger P, Basset-Seguin N, et al. European consensus-based interdisciplinary guideline for melanoma. Part 1: diagnostics: update 2022. Eur J Cancer Oxf Engl. 2022 Jul;1990(170):236–55.
2. Peinado H, Zhang H, Matei IR, Costa-Silva B, Hoshino A, Rodrigues G, et al. Pre-metastatic niches: organ-specific homes for metastases. Nat Rev Cancer. 2017;17(5):302–17.
3. Kaplan RN, Riba RD, Zacharoulis S, Bramley AH, Vincent L, Costa C, et al. VEGFR1-positive haematopoietic bone marrow progenitors initiate the pre-metastatic niche. Nature. 2005;438(7069):820–7.
4. Galli SJ, Borregaard N, Wynn TA. Phenotypic and functional plasticity of cells of innate immunity: macrophages, mast cells and neutrophils. Nat Immunol. 2011;12(11):1035–44.
5. Marichal T, Tsai M, Galli SJ. Mast cells: potential positive and negative roles in tumor biology. Cancer Immunol Res. 2013 Nov;1(5):269–79.
6. Wernersson S, Pejler G. Mast cell secretory granules: armed for battle. Nat Rev Immunol. 2014;14(7):478–94.
7. Gurish MF, Austen KF. Developmental origin and functional specialization of mast cell subsets. Immunity. 2012;37(1):25–33.
8. Aponte-López A, Fuentes-Pananá EM, Cortes-Muñoz D, Muñoz-Cruz S. Mast cell, the neglected member of the tumor microenvironment: role in breast cancer. J Immunol Res. 2018;2018:2584243.
9. Stone KD, Prussin C, Metcalfe DD. IgE, mast cells, basophils, and eosinophils. J Allergy Clin Immunol. 2010;125(2 Suppl 2):S73–80.
10. Öhrvik H, Grujic M, Waern I, Gustafson AM, Ernst N, Roers A, et al. Mast cells promote melanoma colonization of lungs. Oncotarget. 2016;7(42):68990–9001.
11. Wasiuk A, Dalton DK, Schpero WL, Stan RV, Conejo-Garcia JR, Noelle RJ. Mast cells impair the development of protective anti-tumor immunity. Cancer Immunol Immunother CII. 2012 Dec;61(12):2273–82.
12. Michel A, Schüler A, Friedrich P, Döner F, Bopp T, Radsak M, et al. Mast cell-deficient kit(W-sh) 'sash' mutant mice display aberrant myelopoiesis leading to the accumulation of splenocytes that act as myeloid-derived suppressor cells. J Immunol Baltim Md. 2013;190(11):5534–44.
13. Pittoni P, Colombo MP. The dark side of mast cell-targeted therapy in prostate cancer. Cancer Res. 2012 Feb 15;72(4):831–5.
14. Siebenhaar F, Metz M, Maurer M. Mast cells protect from skin tumor development and limit tumor growth during cutaneous de novo carcinogenesis in a kit-dependent mouse model. Exp Dermatol. 2014 Mar;23(3):159–64.
15. Wang Y, Hu L, Zheng Y, Guo L. HMGA1 in cancer: cancer classification by location. J Cell Mol Med. 2019 Apr;23(4):2293–302.
16. Méndez O, Peg V, Salvans C, Pujals M, Fernández Y, Abasolo I, et al. Extracellular HMGA1 promotes tumor invasion and metastasis in triple-negative breast cancer. Clin Cancer Res. 2018;24(24):6367–82.
17. Grimbaldeston MA, Chen CC, Piliponsky AM, Tsai M, Tam SY, Galli SJ. Mast cell-deficient W-sash c-kit mutant kit W-sh/W-sh mice as a model for investigating mast cell biology in vivo. Am J Pathol. 2005;167(3):835–48.
18. Scholten J, Hartmann K, Gerbaulet A, Krieg T, Müller W, Testa G, et al. Mast cell-specific Cre/loxP-mediated recombination in vivo. Transgenic Res. 2008 Apr;17(2):307–15.
19. Biswas A, Richards JE, Massaro J, Mahalingam M. Mast cells in cutaneous tumors: innocent bystander or maestro conductor? Int J Dermatol. 2014 Jul;53(7):806–11.
20. Ribatti D, Ennas MG, Vacca A, Ferreli F, Nico B, Orru S, et al. Tumor vascularity and tryptase-positive mast cells correlate with a poor prognosis in melanoma. Eur J Clin Invest. 2003 May;33(5):420–5.
21. Rajabi P, Bagheri A, Hani M. Intratumoral and peritumoral mast cells in malignant melanoma: an immunohistochemical study. Adv Biomed Res. 2017;6:39.
22. Siiskonen H, Poukka M, Bykachev A, Tyynelä-Korhonen K, Sironen R, Pasonen-Seppänen S, et al. Low numbers of tryptase+ and chymase+ mast cells associated with reduced survival and advanced tumor stage in melanoma. Melanoma Res. 2015;25(6):479–85.
23. Fusco A, Fedele M. Roles of HMGA proteins in cancer. Nat Rev Cancer. 2007;7(12):899–910.
24. Yang M, Guo Y, Liu X, Liu N. HMGA1 promotes hepatic metastasis of colorectal cancer by inducing expression of glucose transporter 3 (GLUT3). Med Sci Monit. 2020;29(26):e924975.
25. Qi C, Cao J, Li M, Liang C, He Y, Li Y, et al. HMGA1 overexpression is associated with the malignant status and progression of breast cancer. Anat Rec Hoboken NJ. 2007;301(6):1061–7.
26. Ohsie SJ, Sarantopoulos GP, Cochran AJ, Binder SW. Immunohistochemical characteristics of melanoma. J Cutan Pathol. 2008;35(5):433–44.
27. Grujic M, Paivandy A, Gustafson AM, Thomsen AR, Öhrvik H, Pejler G. The combined action of mast cell chymase,

tryptase and carboxypeptidase A3 protects against melanoma colonization of the lung. Oncotarget. 2017;8(15):25066–79.

28. Reeves R, Nissen MS. Cell cycle regulation and functions of HMG-I(Y). Prog Cell Cycle Res. 1995;1:339–49.

29. Chiappetta G, Avantaggiato V, Visconti R, Fedele M, Battista S, Trapasso F, et al. High level expression of the HMGI (Y) gene during embryonic development. Oncogene. 1996; 13(11):2439–46.

30. Huang R, Huang D, Dai W, Yang F. Overexpression of HMGA1 correlates with the malignant status and prognosis of breast cancer. Mol Cell Biochem. 2015;404(1–2):251–7.

31. Liau SS, Jazag A, Whang EE. HMGA1 is a determinant of cellular invasiveness and in vivo metastatic potential in pancreatic adenocarcinoma. Cancer Res. 2006;66(24):11613–22.

SUPPORTING INFORMATION

Additional supporting information can be found online in the Supporting Information section at the end of this article.